Stochastic Model of Vesicular Sorting in Cellular Organelles

Quentin Vagne, Pierre Sens

HAL Id: hal-02492121
https://hal.sorbonne-universite.fr/hal-02492121v1

Editors' Suggestion

Stochastic Model of Vesicular Sorting in Cellular Organelles

Quentin Vagne and Pierre Sens

Institut Curie, PSL Research University, CNRS, UMR 168, 26 rue d'Ulm, F-75005 Paris, France

The proper sorting of membrane components by regulated exchange between cellular organelles is crucial to intracellular organization. This process relies on the budding and fusion of transport vesicles, and should be strongly influenced by stochastic fluctuations, considering the relatively small size of many organelles. We identify the perfect sorting of two membrane components initially mixed in a single compartment as a first passage process, and we show that the mean sorting time exhibits two distinct regimes as a function of the ratio of vesicle fusion to budding rates. Low ratio values lead to fast sorting but result in a broad size distribution of sorted compartments dominated by small entities. High ratio values result in two well-defined sorted compartments but sorting is exponentially slow. Our results suggest an optimal balance between vesicle budding and fusion for the rapid and efficient sorting of membrane components and highlight the importance of stochastic effects for the steady-state organization of intracellular compartments.

One important function of membrane-bound intracellular organelles such as the Golgi apparatus or the endosome network is the sorting of membrane components secreted or ingested by the cell [1–3] and their dispatch to appropriate locations via vesicular transport [4]. This process is regulated by molecular recognition during vesicle budding and fusion, permitted by the sensing of membrane composition by coat proteins that control vesicle budding [5,6] and by tethers and SNAREs that mediate vesicle fusion [2,7]. The interplay between vesicle budding and fusion poses a number of interesting questions regarding the dynamics of organelles that robustly maintain distinct compositions while constantly exchanging material. Theoretical studies investigating such questions have mostly focused on steady-state, time-averaged properties of dynamical compartments exchanging material [8–13]. It has been shown in particular that given sufficiently strong specificity of the budding and fusion transport mechanisms, one expects spontaneous symmetry breaking and the appearance of stable compartments with distinct compositions [8,10]. The inherently stochastic nature of intracellular transport has been much less explored [14,15]. Fluctuations should, however, be important, since the typical surface area of an endosome or a Golgi cisterna ($0.2 − 1~\mu m^2$) corresponds to that of a few tens of the transport vesicles (about 50–100 nm in diameter). This explains the fact that strong fluctuations in the size and composition of early endosomes correlate with budding and fusion events [16].

Cellular organelles are highly complex systems receiving, processing, and sorting components. Here, we concentrate on one aspect of this dynamics, which is the sorting of membrane components by means of the emission and

fusion of vesicles targeting specific membrane composition. We develop a fully stochastic description of the process by which two types A and B of membrane components, initially mixed into a single ("mother") compartment, can be sorted into two pure compartments containing only A or B components. The main model ingredients, selective vesicular export and homotypic fusion, are known to play an important role in both endosomes and Golgi dynamics [17]. Our model is of conceptual importance, as it quantifies an important trade-off; homotypic fusion between sorted vesicles is required to form daughter compartments, but back fusion with components still in the mother compartment slows down the sorting process. This suggests the need to optimize the vesicle budding and fusion rates for efficient sorting. Our model is also of practical interest for understanding the transient response of organelles to external perturbations, such as the *de novo* formation of the Golgi apparatus following the redistribution of Golgi proteins to the endoplasmic reticulum (ER) after drug treatment [18,19].

We study the process sketched in Fig. 1, seeking to answer two questions: (i) What is the mean first passage time to the irreversible separation of A and B components? (ii) What is the size distribution of the pure compartments resulting from the sorting process? Organelles are discretized into units of area equal to that of a transport vesicle, so that a given compartment is composed of an integer number N of vesicles. We assume that each unit area has a given composition, and we consider a mixed compartment containing N_A units of type A and N_B units of type B. The fraction of B component in the compartment is written $\phi = N_B/(N_A + N_B)$. We assume that the type-B components are exported by vesicle budding at a rate (per site) that

depends on membrane composition according to a Michaelis-Mentens scheme [20]:

$$K_{\text{site}} = K f(\phi), \qquad f(\phi) \equiv \frac{\phi}{\phi^* + \phi}, \qquad (1)$$

where the parameter K controls the vesicular emission rate and ϕ^* represents the selectivity of vesicle emission for the B component. We show in the Supplemental Material [21] that such kinetics may result from the selective recruitment of B components by membrane-bound vesicle coat components. The situation where both components A and B are exported in the same way is also studied by numerical simulations.

Homotypic fusion between membrane compartments of similar composition controls the dynamics of both the endosomal network [16] and the Golgi apparatus [38]. We implement a general homotypic fusion mechanism based on the idea that any two compartments 1 and 2 of mixed compositions ϕ_1 and ϕ_2 meet at a rate k_f (independent of their size), and they fuse according to the probability that two random sites of their membranes are identical. This leads to the average fusion rate:

$$k_{\text{fusion}} = k_f[\phi_1\phi_2 + (1 - \phi_1)(1 - \phi_2)]. \qquad (2)$$

This homotypic fusion scheme prevents pure A and B compartments (i.e., $\phi_1 = 1$ and $\phi_2 = 0$) from fusing together. Perfect and permanent sorting will thus necessarily occur at some point, after stochastic fluctuations have removed all B components from the mother compartment (see Fig. 1). Below, we derive the mean sorting time both analytically (within some simplifying assumptions) and numerically, and we compute the steady-state size distribution of the sorted compartments.
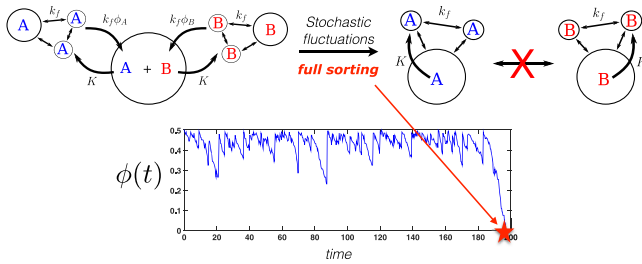

FIG. 1. Sketch of the sorting mechanism. A "mother" compartment contains both A and B membrane components, which are individually exported by vesicle budding (rate K). Secreted vesicles with the same identity fuse with one another to create pure A and B compartments (rate k_f) and may fuse back with the mother compartment with a composition-dependent rate. Pure A and B compartments do not fuse together. Stochastic fluctuations lead to the permanent separation of A and B components into two independent distributions of pure compartments. A typical time trace for the mother compartment composition (with fraction of B component ϕ) is shown. Full sorting occurs when $\phi = 0$ (red star).

Mean sorting time.—We consider that only the B components undergo vesicular sorting, starting from a number N_{B0} of type-B sites in the mother vesicle. In order to make analytical progress, we first assume that all B components removed from the mother compartment aggregate into a single pure-B daughter compartment. This requires us to use an effective budding rate per site smaller than the actual rate $Kf(\phi)$ to account for the back fusion of emitted vesicles with the mother compartment. The effective rate, derived in the Supplemental Material [21], takes the form $Kf'(\phi, k_f/K) = Kf(\phi)[1 - \phi/(1 + \phi + Kf(\phi)/k_f)]$. We compute analytically the mean first passage time (MFPT) to the complete sorting of B components, both in the continuous (infinite-size) limit and taking finite-size effects into account. We then compare these results to numerical simulations that accurately account for the full size distribution of the sorted compartments.

In the large-size limit:($N_B \gg 1$), the fraction $\phi(t)$ of B components in the mother vesicle may be treated as a deterministic continuous variable between fusion events. Its temporal evolution and the time t_0 for complete sorting of B components [corresponding to $\phi(t_0) = 0$] satisfy

$$\frac{d\phi}{dt} = -K(1 - \phi)f'(\phi, k_f/K),$$

$$t_0 = \frac{1}{K}\int_0^{\phi_0} \frac{d\phi}{(1 - \phi)f'(\phi, k_f/K)}. \qquad (3)$$

In addition to the continuous decrease of ϕ through vesicle emission, the compartment containing all the emitted vesicles may fuse back with the mother compartment at any instant with a probability density $k_f\phi(t)$. This defines a stochastic process where $\phi(t)$ continuously decreases towards zero but is submitted to stochastic jumps that reset the system to its initial configuration ϕ_0. Since the total number of jumps is independent of the waiting time before each jump, the MFPT to complete separation may be written

$$\tau = t_0 + \langle n_{\text{jump}} \rangle \langle t_{\text{jump}} \rangle, \qquad (4)$$

where $\langle n_{\text{jump}} \rangle$ is the mean number of jumps and $\langle t_{\text{jump}} \rangle$ is the mean waiting time between two jumps.

As shown in the Supplemental Material [21] [Eq. (S.11)], the mean sorting time can be computed exactly within our approximation, and it shows two qualitatively distinct asymptotic behaviors. When $k_f \ll K$, fusion is very unlikely, and one finds $\tau \simeq t_0$ given by Eq. (3) with $f'(\phi, k_f/K) \approx f(\phi)$. In the other limit, $k_f \gg K$, fusion is frequent, and the mean sorting time approximates to

$$\lim_{k_f \gg K} \tau = \frac{1}{k_f\phi_0} \exp\left(\frac{k_f}{K}\int_0^{\phi_0} d\phi \frac{\phi(1 + \phi)}{(1 - \phi)f(\phi)}\right). \qquad (5)$$

One thus expects a transition between fast sorting and (exponentially) slow sorting when $k_f \simeq K$.

For small systems the continuous approach is not appropriate and must be replaced by the stochastic process:

$$N_B \xrightarrow[\text{budding}]{K(N_B+N_A)f'(\phi,k_f/K)} N_B - 1, \qquad N_B \xrightarrow[\text{fusion}]{k_f\phi} N_{B0}. \quad (6)$$
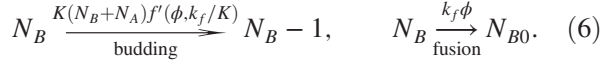
The MFPT τ may be computed exactly for this model as well (see the Supplemental Material [21]), yielding the following asymptotic results in the limits of small and large fusion rates:

$$K\tau \xrightarrow[k_f/K\ll 1]{} \sum_{N_{B}=1}^{N_{B0}} \frac{1}{(N_B + N_A)f(\phi)},$$

$$K\tau \xrightarrow[k_f/K\gg N^2]{} \left(\frac{k_f}{K}\right)^{N_{B0}-1} \prod_{N_B=1}^{N_{B0}} \frac{\phi(1+\phi)/\phi_0}{(N_B + N_A)f(\phi)}, \quad (7)$$

with $\phi = N_B/(N_A + N_B)$. A power-law dependence $K\tau \sim (k_f/K)^{\phi_0 N}$ is predicted in the high fusion regime. There is, however, a crossover region $1 \ll k_f/K \ll N^2$, which is very broad for large systems, between the constant and power-law regimes of sorting time. This region corresponds to the exponential dependency $K\tau \sim e^{k_f/K}$ obtained with the continuous approximation [Eq. (5)].

Numerical simulations of the sorting process were performed following a procedure described in the Supplemental Material [21], in the limit of strong coat selectivity [$\phi^* \ll 1$ in Eq. (1)] to reduce the number of parameters. A typical time trace of the evolution of the compartment composition ϕ is shown in Fig. 1. The dimensionless mean sorting time $K\tau$ (Fig. 2) shows excellent agreement with the analytical results and clearly exhibits the two different sorting regimes predicted analytically. Numerical studies of more realistic models, where the sorting vesicles are composed of a large number of small membrane patches and where one species may contaminate (with a low probability) the vesicles exporting the other species, are presented in the Supplemental Material [21]. They also show the existence of the two sorting regimes, with the same crossover as the simpler model.

The crossover value of k_f/K at which the dynamical transition between fast and slow sorting occurs can be obtained from mean field arguments. Sorting is a slow process if the system reaches a long-lived steady state where the fusion of the sorted compartments with the mother compartment balances vesicle budding. We write a dynamical equation for the average number N_B of B components in the mother compartment that includes its decrease because of vesicle budding [at a rate $K(N_A + N_B)f(\phi)$] and its increase by fusion with the $N_{B0} - N_B$ sorted components (at a rate $k_f\phi$):
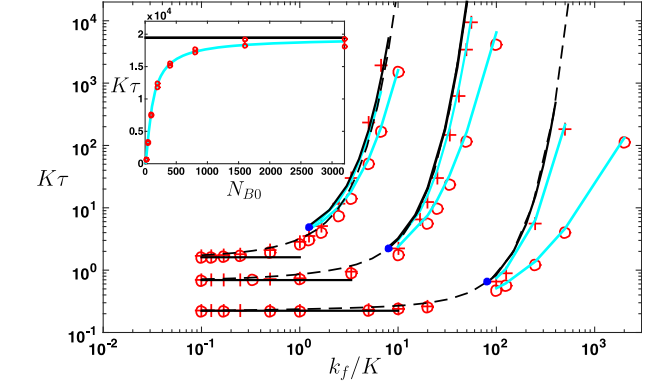

FIG. 2. Dimensionless mean first passage time $K\tau$ as a function of the ratio of fusion to budding rate k_f/K for different initial compositions and sizes. The three groups of curves correspond to different initial compositions (from left to right: $\phi_0 = 0.8$, 0.5, and 0.2). The simulation results are shown for two different initial compartment sizes in each case (red circles: $N_0 = 20$; red crosses: $N_0 = 100$). The black curves show the analytical results for $N_0 \to \infty$, the dashed line is the full solution [Eq. (S.11) in the Supplemental Material [21]], and solid lines are the asymptotic limits for $K \gg k_f$ (t_0) and $K \ll k_f$ [Eq. (5)]. The light blue curves show the results of the discrete model [Eq. (7)]. The crossover from fast to slow sorting [Eq. (9)] is shown with blue dots. Inset: Size dependence of the mean first passage time $K\tau$ (with $\phi_0 = 0.5$ and $k_f/K = 50$). The error bars are standard deviations over many independent simulations.

$$\dot{N}_B = -K(N_A + N_B)f(\phi) + k_f \frac{N_B}{N_A + N_B}(N_{B0} - N_B). \quad (8)$$

As discussed in the Supplemental Material [21], in the limit $\phi^* \ll \phi_0$ that interests us here, Eq. (8) admits a stable steady state with $N_B \neq 0$ only if

$$\frac{k_f}{K} \geq \frac{4(1 - \phi_0)}{\phi_0^2}. \quad (9)$$

This condition quantitatively predicts the crossover between fast and slow sorting (shown by blue dots in Fig. 2). This result can be extended to the case where both A and B components can bud from the compartment. The transition from fast to slow sorting in this case is shown in Fig. 3(b). For an initially symmetric compartment ($N_{A0} = N_{B0}$), it occurs when $k_f/K \geq 1/4$.

Size distribution of the sorted compartments.—Although it provides an accurate description of the different regimes of sorting dynamics and their crossover (Fig. 2), the assumption that all emitted vesicles gather into a single compartment is clearly an oversimplification, and one expects a distribution of size for the sorted compartments. Analytically solving the full sorting problem while accounting for this dynamically varying size distribution is very challenging. One may, however, understand the role of budding and fusion on the compartment size distribution by investigating the steady-state size distribution of the
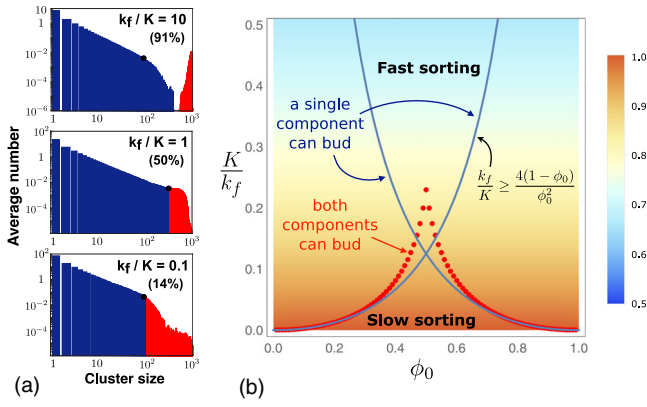
FIG. 3. (a) Steady-state size distribution of one-component compartments undergoing fusion at a rate k_f and shedding vesicles at a rate K, for different values of the fusion to budding-rate ratio k_f/K. The total membrane area is $N = 10^3$. The single largest compartment corresponds to the red part of the distribution, whose integral equals unity. It contains a fraction ρ of the total area, given in parentheses, consistent with Eq. (11). The typical size of the small compartments, obtained in the Supplemental Material [21], is displayed on each graph (black dots). (b) Sorting phase diagram showing how the interplay between vesicular export and fusion influences both the sorting time and the distribution of sorted components. The color background represents the fraction ρ of the total area contained in the largest compartment. The boundary between fast and slow sorting is indicated by the solid blue lines when only one component can be exported in budding vesicles [Eq. (9)], and by the red dotted line when both components can be exported.

fully sorted B components, which are then isolated from the mother compartment. At the mean field level, the number N_n of pure B compartments of size n evolves via vesicle budding and compartment fusion according to the master equation [11,39]

$$\frac{dN_n}{dt} = \frac{k_f}{2} \sum_{m=1}^{n-1} N_m N_{n-m} - k_f N_n \sum_{m=1}^{\infty} N_m$$
$$+ K(n+1)N_{n+1} - K n N_n + \delta_{n,1} K \sum_{m=1}^{\infty} N_m m, \quad (10)$$

with the constraint that the total amount of B components is fixed: $\sum_{n=1}^{\infty} n N_n = N_{B0}$.

The steady-state solution of Eq. (10), studied in the Supplemental Material [21], shows a typical power-law decay with an exponential cutoff size. Numerical simulations [Fig. 3(a)] show the failure of the mean field approach for fast fusion rates: $k_f/K > 1$, and the appearance of a single macrocompartment containing most of the components. This can be understood qualitatively: for a compartment of size n, balancing the evaporation rate $(= Kn)$ and the average growth rate by fusion $(\simeq k_f \sum_m m N_m = N_{B0} k_f)$ yields a stationary size $n = N_{B0} k_f/K$, consistent with the exact solution of Eq. (10) derived in the Supplemental Material [21] if $k_f/K \ll 1$. If

$k_f/K \geq 1$, this predicts a compartment size larger than the total system's mass, indicating the failure of the mean field equation (10). Assuming a macrocompartment emerges in this case and contains a fraction ρ of the total mass N_{B0}, balancing its growth by fusion with smaller compartments [flux $k_f(1-\rho)N_{B0}$] and its shrinkage by budding (flux $K\rho N_{B0}$) yields

$$\rho = \frac{k_f}{k_f + K}. \quad (11)$$

Equation (11) is in good quantitative agreement with the result from the full-size distribution computed numerically and shown in Fig. 3(a). We stress that the formation of a macrocompartment described here is a stochastic phenomenon related to finite-size effects, and that it is robust upon variation of the fusion kernel in Eq. (10) (see the Supplemental Material [21]). It is thus distinct from the mean field gelation phenomenon, which crucially depends on the size dependency of the fusion kernel [40,41].

Discussion.—The previous results show that the sorting of membrane components via selective (composition-dependent) budding and fusion events is best achieved for intermediate values of the ratio of fusion to budding rates, k_f/K. In the absence of fusion, the composition of the mother compartment in a given component (B, say) removed by vesicle budding decreases with a time scale equal to the inverse budding rate. Sorting is thus very fast, but the sorted component ends up dispersed in a large number of small vesicles that are unable to fuse with one another. If fusion is allowed between membrane sites sharing the same identity, the budded vesicles are able to fuse with one another and form large compartments made solely of the sorted (B) components. However, fusion of the B components back with the mother compartment dramatically slows down the sorting process. The resulting sorting time then strongly depends on the ratio of fusion to budding rate. The dependency is exponential for large compartments, and is a power law for small compartments [Eqs. (5) and (7)]. There is thus a clear optimization problem to solve in order to obtain two (or a few) well-sorted compartments containing only A or B components in a relatively short time. This is illustrated in Fig. 3(b), where the boundaries between fast and slow sorting regimes are shown, together with the fraction of the sorted components that are contained within a single, large compartment.

Within this model, fast sorting of a binary mixture of membrane components of arbitrary composition is compatible with the existence of macrocompartments containing up to 80% of the sorted components. Physiologically, exchange rates between organelles vary widely, which justifies our "phase diagram" approach to explore the full range of possible dynamical behavior. Budding rates of order $K \simeq 10^{-2}$/s have been reported for the Golgi [42]. Similar rates can be inferred from the bulk flow leaving ER exit sites [43,44]. Fusion rates are more difficult to estimate. An upper

bound of 1/s is obtained by considering the time needed for a vesicle diffusing at 1 $\mu m^2/s$ to explore the typical Golgi dimension (1 μm). Choosing a typical ratio $K/k_f \simeq 0.03$ yields fast sorting ($\lesssim 10$ s) for $\phi_0 < 0.3$ and exponentially slow for $\phi_0 > 0.3$. Experimentally, *de novo* Golgi biogenesis after BFA-induced Golgi redistribution into the ER appears slow ($\simeq 20$ min [19]). Within our model, this corresponds to the redistributed Golgi accounting for a fraction $\phi_0 = 0.45$ of the ER.

While organelles along the cell trafficking pathways may to some extent be viewed as a steady state of a complex dynamical system, specific budding and fusion events, which are at the heart of their organization, are inherently stochastic processes. The relatively slow dynamics of *de novo* Golgi formation from the ER [19], as compared to the rate of ER vesiculation, suggests the existence of kinetic barriers that must be overcome stochastically. The strong fluctuations of the size and composition of early endosomes, before stochastic fluctuations lead to their full maturation into late endosomes [16], is another illustration of the need for a stochastic treatment of intracellular transport for physiologically relevant values of the exchange rates controlling intracellular organization. The present study proposes such a stochastic model for the process of vesicular sorting. Beyond its importance for identifying an optimal range of fusion to budding rate for efficient sorting, our formalism constitutes a general framework that can be used to study more complex situations of relevance to the dynamics of cellular organelles, such as the case where membrane components undergo biochemical transformation [45].

[1] I. Mellman, Endocytosis and molecular sorting, Annu. Rev. Cell Dev. Biol. **12**, 575 (1996).

[2] H. Cai, K. Reinisch, and S. Ferro-Novick, Coats, tethers, rabs, and snares work together to mediate the intracellular destination of a transport vesicle, Dev. Cell **12**, 671 (2007).

[3] M. Jovic, M. Sharma, J. Rahajeng, and S. Caplan, The early endosome: A busy sorting station for proteins at the crossroads Histology histopathol. **25**, 99 (2010).

[4] R. Kelly, Pathways of protein secretion in eukaryotes, Science **230**, 25 (1985).

[5] J. Mancias and J. Goldberg, Structural basis of cargo membrane protein discrimination by the human COPII coat machinery, EMBO J. **27**, 2918 (2008).

[6] L. Traub, Tickets to ride: Selecting cargo for clathrin-regulated internalization, Nat. Rev. Mol. Cell Biol. **10**, 583 (2009).

[7] Y. Chen and R. Scheller, SNARE-mediated membrane fusion, Nat. Rev. Mol. Cell Biol. **2**, 98 (2001).

[8] R. Heinrich and T. A. Rapoport, Generation of nonidentical compartments in vesicular transport systems, J. Cell Biol. **168**, 271 (2005).

[9] B. Binder, A. Goede, N. Berndt, and H. Holzhutter, A conceptual mathematical model of the dynamic self-organisation of distinct cellular organelles, PLoS One **4**, e8295 (2009).

[10] S. Dmitrieff and P. Sens, Cooperative protein transport in cellular organelles, Phys. Rev. E **83**, 041923 (2011).

[11] L. Foret, J. Dawson, R. Villaseñor, C. Collinet, A. Deutsch, L. Brusch, M. Zerial, Y. Kalaidzidis, and F. Jülicher, A general theoretical framework to infer endosomal network dynamics from quantitative image analysis, Curr. Biol. **22**, 1381 (2012).

[12] P. C. Bressloff, Two-pool model of cooperative vesicular transport, Phys. Rev. E **86**, 031911 (2012).

[13] I. Ispolatov and A. Müsch, A model for the self-organization of vesicular flux and protein distributions in the Golgi apparatus, PLoS Comput. Biol. **9**, e1003125 (2013).

[14] H. Gong, Y. Guo, A. Linstedt, and R. Schwartz, Discrete, continuous, and stochastic models of protein sorting in the Golgi apparatus, Phys. Rev. E **81**, 011914 (2010).

[15] P. Bressloff and J. Newby, Stochastic models of intracellular transport, Rev. Mod. Phys. **85**, 135 (2013).

[16] J. Rink, E. Ghigo, Y. Kalaidzidis, and M. Zerial, Rab conversion as a mechanism of progression from early to late endosomes, Cell **122**, 735 (2005).

[17] J. Bonifacino and B. Glick, The mechanisms of vesicle budding and fusion, Cell **116**, 153 (2004).

[18] B. Glick, Can the Golgi form de novo? Nat. Rev. Mol. Cell Biol. **3**, 615 (2002).

[19] S. Puri and A. Linstedt, Capacity of the Golgi apparatus for biogenesis from the endoplasmic reticulum, Mol. Biol. Cell **14**, 5011 (2003).

[20] K. A Johnson and R. S Goody, The original Michaelis constant: Translation of the 1913 Michaelis–Menten Paper, Biochemistry **50**, 8264 (2011).

[21] See the Supplemental Material at http://link.aps.org/supplemental/10.1103/PhysRevLett.120.058102 for additional computations and analysis, which includes Refs. [22–37].

[22] D. Loerke, M. Mettlen, D. Yarar, K. Jaqaman, H. Jaqaman, G. Danuser, and S. Schmid, Cargo and dynamin regulate clathrin-coated pit maturation, PLoS Biol. **7**, e1000057 (2009).

[23] R. Forster, M. Weiss, T. Zimmermann, E. Reynaud, F. Verissimo, D. Stephens, and R. Pepperkok, Secretory cargo regulates the turnover of COPII subunits at single ER exit sites, Curr. Biol. **16**, 173 (2006).

[24] L. Foret and P. Sens, Kinetic regulation of coated vesicle secretion, Proc. Natl. Acad. Sci. U.S.A. **105**, 14763 (2008).

[25] N. G. V. Kampen, *Stochastic Processes in Physics and Chemistry* (Elsevier, New York, 1992).

[26] I. Simon, M. Zerial, and R. S. Goody, Kinetics of interaction of Rab5 and Rab7 with nucleotides and magnesium ions, J. Biol. Chem. **271**, 20470 (1996).

[27] S. Takamori *et al.*, Molecular anatomy of a trafficking organelle, Cell **127**, 831 (2006).

[28] H. Galina and J. B. Lechowicz, Mean-field kinetic modelling of polymerization: The Smoluchowski coagulation equation, Adv. Polym. Sci. **137**, 135 (1998).

[29] S. C. Davies, J. King, and J. Wattis, Self-similar behaviour in the coagulation equations, J. Eng. Math. **36**, 57 (1999).

[30] P. L. Krapivsky and S. Redner, Transitional aggregation kinetics in dry and damp environments, Phys. Rev. E **54,** 3553 (1996).

[31] R. Rajesh and S. N. Majumdar, Exact phase diagram of a model with aggregation and chipping, Phys. Rev. E **63,** 036114 (2001).

[32] M. Abramowitz and I. A. Stegun, *Handbook of Mathematical Functions.* (Dover, New York, 1964).

[33] Q. Vagne, M. Turner, and P. Sens, Sensing size through clustering in nonequilibrium membranes and the control of membrane-bound enzymatic reactions, PLoS One **10,** e0143470 (2015).

[34] M. H. Lee, A survey of numerical solutions to the coagulation equation, J. Phys. A **34,** 10219 (2001).

[35] C. Connaughton, R. Rajesh, and O. Zaboronski, Stationary Kolmogorov solutions of the Smoluchowski aggregation equation with a source term, Phys. Rev. E **69,** 061114 (2004).

[36] J. Camacho, Scaling in steady-state aggregation with injection, Phys. Rev. E **63,** 046112 (2001).

[37] D. Gillespie, Exact stochastic simulation of coupled chemical reactions, J. Chem. Phys. **81,** 2340 (1977).

[38] S. Pfeffer, How the Golgi works: A cisternal progenitor model, Proc. Natl. Acad. Sci. U.S.A. **107,** 19614 (2010).

[39] M. S. Turner, P. Sens, and N. D. Socci, Nonequilibrium Raftlike Membrane Domains under Continuous Recycling, Phys. Rev. Lett. **95,** 168301 (2005).

[40] M. Ernst, *Fractals in Physics*, edited by L. Pietronero and E. Tosatti (North-Holland, Amsterdam, 1986).

[41] F. Leyvraz, Scaling theory and exactly solved models in the kinetics of irreversible aggregation, Phys. Rep. **383,** 95 (2003).

[42] Y. Wang, J.-H. Wei, B. Bisel, D. Tang, and J. Seemann, Golgi cisternal unstacking stimulates COPI vesicle budding and protein transport, PLoS One **3,** e1647 (2008).

[43] F. Thor, M. Gautschi, R. Geiger, and A. Helenius, Bulk flow revisited: Transport of a soluble protein in the secretory pathway, Traffic **10,** 1819 (2009).

[44] A. Budnik and D. J. Stephens, ER exit sites: Localization and control of COPII vesicle formation, FEBS Lett. **583,** 3796 (2009).

[45] Q. Vagne and P. Sens (to be published).